Arrangement of multiple structural units in a [0001] Σ49 tilt grain boundary in ZnO

Yukio Sato,[1] Teruyasu Mizoguchi,[2] Fumiyasu Oba,[3] Yuichi Ikuhara,[2] and Takahisa Yamamoto[1,*]
[1]*Department of Advanced Materials Science, The University of Tokyo, 5-1-5 Kashiwanoha, Kashiwa, Chiba 277-8651, Japan*
[2]*Institute of Engineering Innovation, The University of Tokyo, 2-11-16 Yayoi, Bunkyo-ku, Tokyo 113-8656, Japan*
[3]*Department of Materials Science and Engineering, Kyoto University, Yoshida-Honmachi, Sakyo-ku, Kyoto 606-8501, Japan*
(Received 22 March 2005; revised manuscript received 13 June 2005; published 16 August 2005)

Arrangement of structural units in a ZnO [0001] Σ=49 symmetric tilt boundary was investigated using a combination of high-resolution electron microscopy and atomistic calculation in detail. The boundary is found to be described by the combination of two different dislocationlike structural units and a bulklike structural unit. The two dislocationlike units were very similar to structural units found in a Σ=7 boundary. One of the dislocationlike units contains threefold-coordinated atoms and the other one has fivefold-coordinated atoms in contrast to fourfold coordination in ZnO bulk. Interestingly, the Σ=49 boundary dominantly consists of a straight alternate array of dislocationlike units and a bulklike unit. A zigzag array of the units partly appeared, which can be related to the straight array via atom flipping at the boundary core. It is considered that the alternate array of dislocationlike units effectively relaxes local strain in the vicinity and, hence, minimizes the boundary energy.

DOI: 10.1103/PhysRevB.72.064109 PACS number(s): 68.35.−p, 68.37.Lp

I. INTRODUCTION

Physical properties in polycrystalline materials are often influenced by the grain boundaries, and the importance of grain boundary atomic structure has been stimulating a large number of studies. Both experimental and theoretical techniques have revealed grain boundary atomic structure in many kinds of crystalline materials, such as metals and metal oxides.[1–18] Through a number of studies, the structural unit model has been proposed and developed to describe systematical change in grain boundary atomic structure with macroscopic degrees of freedom, i.e., misorientation or inclination.[19–24] In the structural unit model, grain boundary atomic structure can be described by the array of fundamental units (structural units). For example, atomic structure of several [110] tilt boundaries in Al can be systematically described by the combination of the structural units.[22,23] An understanding of detailed arrangements of the structural units is very important to know the nature of grain boundary atomic structures. However, it seems that arguments about arrangement of the structural units have been limited so far, especially for oxide materials.

ZnO is one of the most promising oxide materials for light-emitting and transparent electronic devices because of its substantial advantages in these applications.[25–29] Since the grain boundaries generally degrade the optical and/or electrical properties of ZnO, their detailed structure must be understood at atomistic and electronic levels to improve their properties. On the other hand, the grain boundaries in polycrystalline ZnO are well known to show one of the most important properties: highly nonlinear current-voltage characteristics.[30–34] These characteristics have been widely utilized to protect electronic devices as varistors. It is also important to understand the generation mechanism of the varistor property. In order to clarify the generation mechanism, the understanding of the grain boundary atomic structure should be indispensable.

The atomic structures in some of ZnO [0001] tilt boundaries have been investigated in previous studies.[35–38] The boundaries were found to have various coordinated (from fourfold- to tenfold-coordinated) open channels, which are particular to their proper structural units.[35–37] The presence of such various coordinated open channels changed the coordination numbers of specific atomic columns.[37] Recently, it was reported that the atomic structure of [0001] tilt boundaries can be described by the combination of multiple structural units.[37] However, it has not been understood how the multiple structural units arrange along the boundaries. This should be very important to understand the atomic structure of general ZnO grain boundaries. In the present study, a ZnO [0001] Σ=49 symmetric tilt boundary was investigated. The atomic structure of the boundary was revealed using a combination of high-resolution electron microscopy and atomistic calculation. The Σ=49 boundary with a relatively large Σ value is selected, as it has a relatively long periodicity unit. The boundary is expected to include some structural units in the long periodicity unit, which is suited to investigate the arrangement of multiple structural units.

II. EXPERIMENTAL AND COMPUTATIONAL PROCEDURES

A. Experimental procedure

A [0001] Σ=49 symmetric tilt grain boundary was fabricated in a ZnO bicrystal as schematically shown in Fig. 1. The tilt angle, which is made by the $[1\bar{1}00]$ direction of two crystals, is 16.4° and the boundary plane is $(35\bar{8}0)$. The bicrystal was fabricated by hot-pressing two ZnO single crystals (99.99%, Furuuchi Chem. Co., Ltd.) at 1100 °C for 10 h in air under a uniaxial load of 1.5 MPa. The fabrication procedure has been previously described in detail.[39]

Several slices were cut from the ZnO bicrystal for transmission electron microscopy (TEM) observations. The slices were mechanically polished and dimpled down to about 20 μm and finally thinned by an argon-ion beam (PIPS,

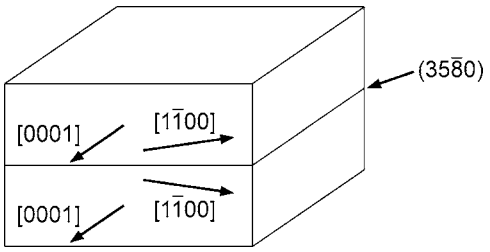

FIG. 1. Schematic of the ZnO bicrystal fabricated in the present study. Common rotation axes of both crystals are [0001], and boundary planes are composed of (35$\bar{8}$0) of both crystals. A tilt angle of the boundary, which is made by [1$\bar{1}$00] of both crystals, is 16.4°.

Gatan Co., Ltd.) with gun voltages of 2–4 kV and beam angles of 6°–7° to make an electron transparency. The boundary was observed from the [0001] direction of both crystals using conventional and high-resolution TEM (JEM-2010HC and JEM-4010, operated at 200 and 400 kV, JEOL Co., Ltd.).

B. Computational procedure

Atomistic calculations were separately performed to theoretically predict stable boundary atomic structures. Similar to our previous studies,[37,38,40] the atomic structures were modeled by the lattice-statics method with the GULP program code.[41] Buckingham-type two-body ionic potentials were employed with the potential parameters reported by Lewis and Catlow.[42] The validity of the potential parameters has been confirmed by the agreement with experimental lattice and elastic constants of ZnO.[38]

The lattice-statics calculations were made using supercells containing initial structure of two same [0001] $\Sigma=49$ boundaries. Two boundaries were set in the supercell by pairing two half-crystal cells with (35$\bar{8}$0) surfaces. An example of the half-crystal cell is shown in Fig. 2. As recognized in the figure, there are two different termination planes for the (35$\bar{8}$0) surface in ZnO with wurtzite crystal structure

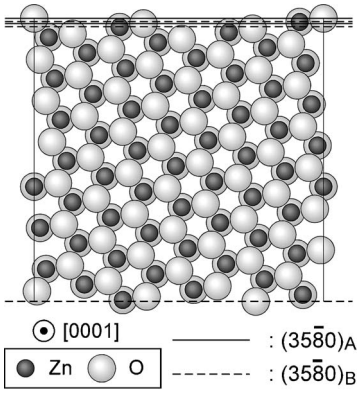

FIG. 2. Example of a half-crystal cell with (35$\bar{8}$0) surfaces. Here, an upper and a lower side of the half-crystal is terminated with (35$\bar{8}$0)$_A$ and (35$\bar{8}$0)$_B$, respectively. Solid horizontal lines indicate (35$\bar{8}$0)$_A$ and dotted ones show (35$\bar{8}$0)$_B$ in the figure.

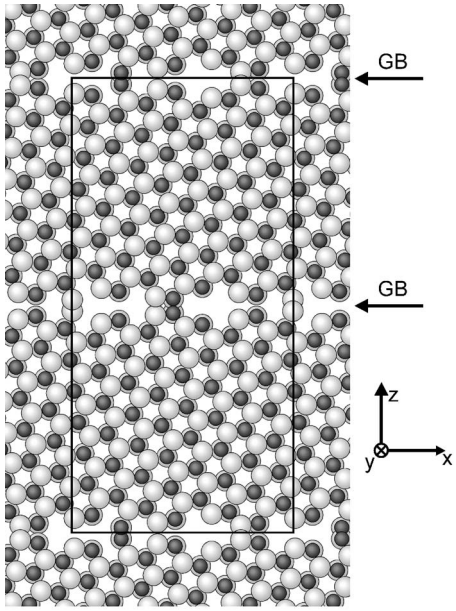

FIG. 3. Example of a supercell used in the atomistic calculation. Here, the boundary planes were composed of terminations of (35$\bar{8}$0)$_B$ and (35$\bar{8}$0)$_B$. Initial structures with a translation state of 0 nm in both the x and y directions and 0.1 nm in the z direction are shown in the figure. Rectangles show the initial supercell and arrows indicate the positions of grain boundaries.

[(35$\bar{8}$0)$_A$ and (35$\bar{8}$0)$_B$]. In the present calculation, three types of boundary models were considered, where combinations of the two same or two different (35$\bar{8}$0) planes compose the boundary planes: (35$\bar{8}$0)$_A$ and (35$\bar{8}$0)$_A$, (35$\bar{8}$0)$_A$ and (35$\bar{8}$0)$_B$, and (35$\bar{8}$0)$_B$ and (35$\bar{8}$0)$_B$. Figure 3 shows an example of the supercell, where (35$\bar{8}$0)$_B$ and (35$\bar{8}$0)$_B$ compose the boundary plane. Supercells with a number of initial structures, in which one half-crystal was three dimensionally translated relative to the other one, were prepared. In the x and z directions, translation states with increments of 0.02 and 0.01 nm were considered. On the other hand, translations of zero and a half of a ZnO unit cell (about 0.26 nm) were taken into account in the y direction (corresponding to the [0001] direction in ZnO), because optimized structures were found only from these two translations in our previous study on a $\Sigma=7$ boundary with the same rotation axis of [0001].[38] In addition, basal planes of two adjacent crystals can be connected without any deviations only in the two translations, which would cause a reduction of total lattice energy to form a stable structure. Boundary expansion was considered as the translation in the z direction. The translation state in the z direction is defined to be zero, when the interfacial spacing between upper and lower half-crystal cells is the same as a half of the interplanar spacing between neighboring (35$\bar{8}$0)$_A$. This corresponds to the average spacing between the neighboring (35$\bar{8}$0)$_A$ and (35$\bar{8}$0)$_B$. Since distances between two parallel boundaries in the supercells should be long enough to avoid interaction between the boundaries, the distances were set to be about 2.2 nm, which are similar to our previous study with the same calculation method.[37] As a result,

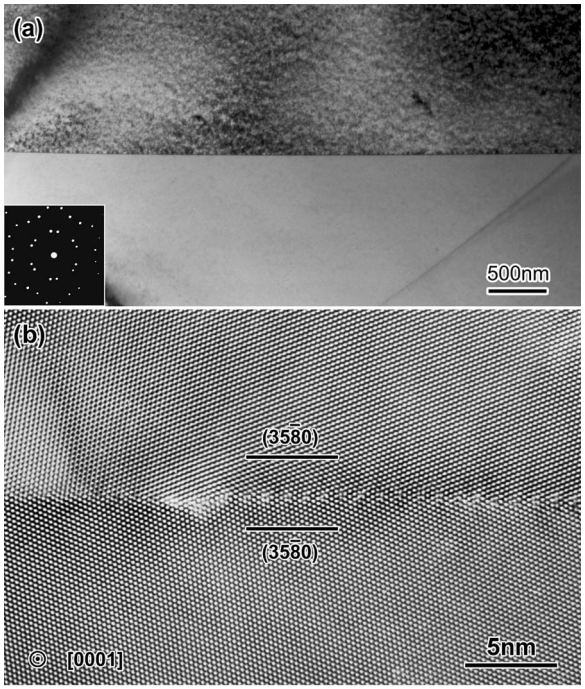

FIG. 4. (a) TEM bright field image and (b) HRTEM image of the $\Sigma=49$ boundary in the ZnO bicrystal. A selected area diffraction pattern obtained from the boundary region is shown in the inset in (a). An incident electron beam in (a) is slightly misaligned from the common [0001] direction to make the contrast difference between both crystals.

the supercells contain 440–456 atoms. Respective atomic positions were optimized so as to minimize the total lattice energy under three dimensionally periodic boundary and constant volume conditions. Energetically favorable atomic structures can thus be obtained in the present study. In addition, initial structures with certain atomic columns added or removed from the obtained stable structures were investigated to find other possible stable structures, since these atomic structures are different from those obtained through the simple translation. Boundary energy was also evaluated as a function of the three-dimensional translations.

Finally, theoretically calculated stable structures were compared to the experimental high-resolution TEM (HRTEM) images. HRTEM image simulations were conducted for the calculated structures using the TEMPAS program code[43] based on the multislice method.[44] HRTEM images were systematically simulated as a function of defocus and specimen thickness to yield an appropriate match to experimental images.

III. RESULTS AND DISCUSSIONS

A. Dominant structure: straight array of structural units

Figure 4 shows TEM bright field and HRTEM images of the $(35\bar{8}0)$ $\Sigma=49$ boundary. There are no intergranular phases such as an amorphous film at the boundary and two ZnO single crystals were joined smoothly at the atomic level. The inset in Fig. 4(a) is a selected area diffraction pattern

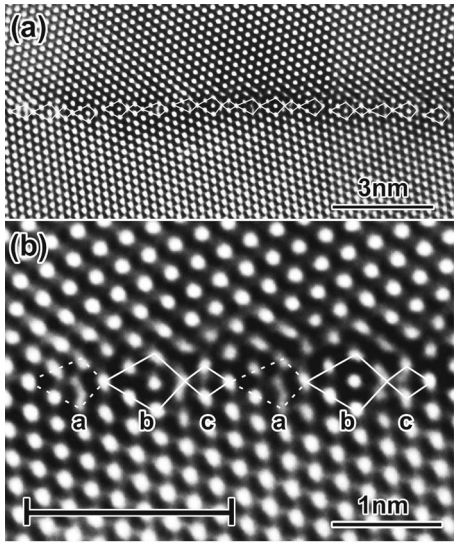

FIG. 5. (a) A HRTEM image showing an array of dislocationlike (larger quadrilaterals) and bulklike (smaller quadrilaterals) units and (b) the magnified HRTEM image showing the straight alternate array of dislocationlike units and a bulklike unit (the unit **c**). The periodicity unit of the boundary is indicated in the lower part of (b). Two different dislocationlike units, which are denoted by dotted (the unit **a**) and solid larger (the unit **b**) quadrilaterals, are clearly observed in (b).

obtained from the region including both crystals. From the diffraction pattern, a tilt angle of the boundary was estimated at $\sim 16.4°$, which is almost the same as the intended orientation in the fabricated bicrystal.

From a detailed analysis of the HRTEM image, the boundary was found to be described by the array of structural units. To clarify this, an enlargement of the part in the HRTEM image is shown in Fig. 5(a), where the structural units are designated by quadrilaterals. The smaller ones correspond to the unit cell of ZnO with some distortion, as illustrated by modeled atomic structures shown later in Fig. 6(a). They will be denoted as bulklike units (**c**) hereafter. The larger ones are different from the smaller and hence particular to the grain boundary. In our previous study, similar structural units were observed at other [0001] tilt grain boundaries in ZnO.[37] These units were found to be very similar to the structures of edge dislocations,[37] and will be denoted as dislocationlike units in this paper.

Figure 5(b) shows the magnified HRTEM image of the array of straightly aligned structural units in Fig. 5(a). In the figure, noticeable differences can be recognized among the dislocationlike units. Some of the units (dotted quadrilaterals; **a**) show the following imaging features: weaker contrast at the center and a circular spot on the right-hand corners. The other units (solid large quadrilaterals; **b**) differ in some points; there is a circular bright spot at the center and a U-shaped elongated spot on the right-hand corner. Thus, the two units are expected to have different atomic structures. Another interesting thing featured by Fig. 5(b) is that the periodicity unit of the boundary, represented by the two dislocationlike units plus one bulklike unit, contains two kinds of dislocationlike units. That is, the periodicity unit is com-

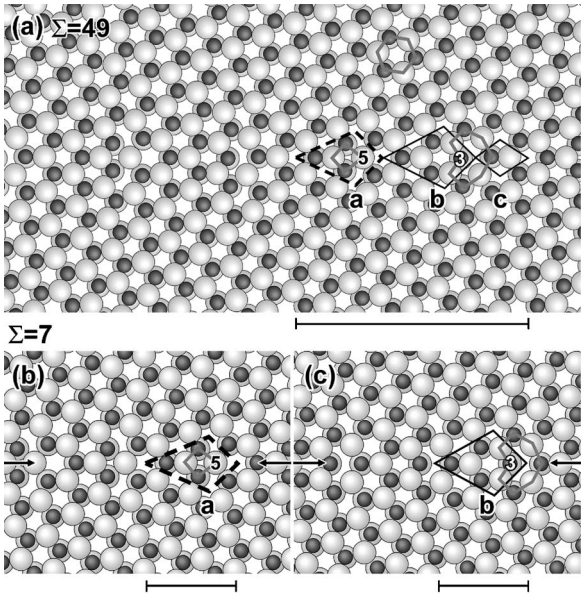

FIG. 6. (a) Most stable structure of the $\Sigma=49$ boundary obtained by the present atomistic calculations. (b), (c) Stable structures of a $\Sigma=7$ boundary reported in Ref. 37. Position of the boundaries is indicated by arrows. Dotted and solid large (black) quadrilaterals show the dislocationlike units and solid small (black) one shows a bulklike unit. A periodicity unit of each boundary is indicated in the lower part of the figures. Atoms marked with 3 and 5 indicate undercoordinated (threefold-coordinated) and overcoordinated (fivefold-coordinated) atoms in contrast to fourfold-coordination ZnO in the bulk. As a result, a small fourfold-coordinated channel in the unit **a** and an eightfold-coordinated channel in the unit **b** are formed, which are shown by gray polygons. For comparison, a sixfold-coordinated open channel in ZnO bulk is also indicated by a gray hexagon in (a).

posed of **a**+**b**+**c** as clearly recognized in the figure. Extensive HRTEM observation indicated that this is a dominant structure in the present $\Sigma=49$ boundary.

Figure 6(a) shows the most stable structures obtained by the present atomistic calculation. This structure has a boundary energy of 1.25 J/m^2, which is the lowest among the structures modeled in the present calculation. This structure was obtained from the termination of $(35\bar{8}0)_B$ and $(35\bar{8}0)_B$ and the translation state of 1.18 nm along the x direction and 0 nm in the y and z directions. The boundary energy of 1.25 J/m^2 is lower than those of stable structures in the $\Sigma=7$ boundary (1.54 J/m^2) obtained by the same method.[37] This is considered to be due to the lower density of atoms with different coordination number from the perfect crystal. It has been reported that grain boundary energy in yttria-stabilized cubic zirconia can be related to the density of atoms with different coordination number.[45] In the modeled structure of the $\Sigma=49$ boundary, the density of atoms with different coordination number is about 3.4/nm^2, which is lower than that of a $\Sigma=7$ boundary, about 4.6/nm^2.[37]

In detail, the modeled $\Sigma=49$ boundary is composed of **a**+**b**+**c** as in the case of the experimentally observed structure. Detailed comparison revealed that **a** is very similar to one of those in the $\Sigma=7$ boundary modeled by the same

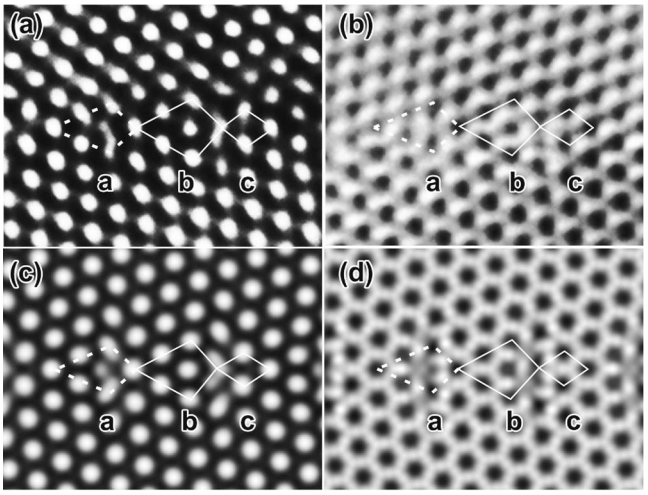

FIG. 7. Comparison between experimental and simulated HRTEM images. (a) An enlarged experimental image of straight array of the units. (b) Another experimental image obtained from the same region but under a different defocus. (c) and (d) Simulated images based on the calculated structure as in Fig. 4(a). (c) A simulated image with a specimen thickness of 4 nm and a defocus of −28 nm. (d) Another simulated image with a thickness of 4 nm and a defocus of −78 nm. These imaging conditions were found to give the best matches to the images shown in (a) and (b). Quadrilaterals indicate the dislocationlike and bulklike units.

method[37] [Fig. 6(b)] and **b** is also close to the other one in the $\Sigma=7$ boundary [Fig. 6(c)]. The former has overcoordinated (labeled with the coordination number 5 in the figure) and the latter contains undercoordinated atoms (labeled with the coordination number 3 in the figure). All other atoms have fourfold coordination as in the ZnO perfect crystal. Correspondingly, fourfold-coordinated small open channel and eightfold-coordinated open channel are formed along the [0001] direction in **a** and **b**, respectively. These are in contrast to the sixfold-coordinated channels recognized in the grain interior.

Figure 7 shows a comparison between the experimentally observed HRTEM images and simulated images based on the calculated stable structure in Fig. 6(a). Figures 7(a) and 7(b) show the experimental images obtained from the same area with different imaging conditions. For the image in (a), the simulated image with a specimen thickness of 4 nm and a defocus of −28 nm [Fig. 7(c)] was found to give the best match to this experimental image. On the other hand, the simulated image with a specimen thickness of 4 nm and a defocus of −78 nm [Fig. 7(d)] yielded an appropriate match to the image shown in Fig. 7(b). Since the features of experimental images under two defocus conditions are well reproduced by the simulated images, the atomic structure as shown in Fig. 6(a) is assumed to be actually observed.

Atomic structures of the $\Sigma=49$ $(35\bar{8}0)$ boundary in GaN, which has the same wurtzite structure as ZnO, have been also reported through atomistic calculations.[46,47] Similar to the present result, the structures contain two dislocationlike units and one bulklike unit. However, the detailed atomic structure seems different from the present result. The GaN $\Sigma=49$ boundaries contain the units that are characterized by

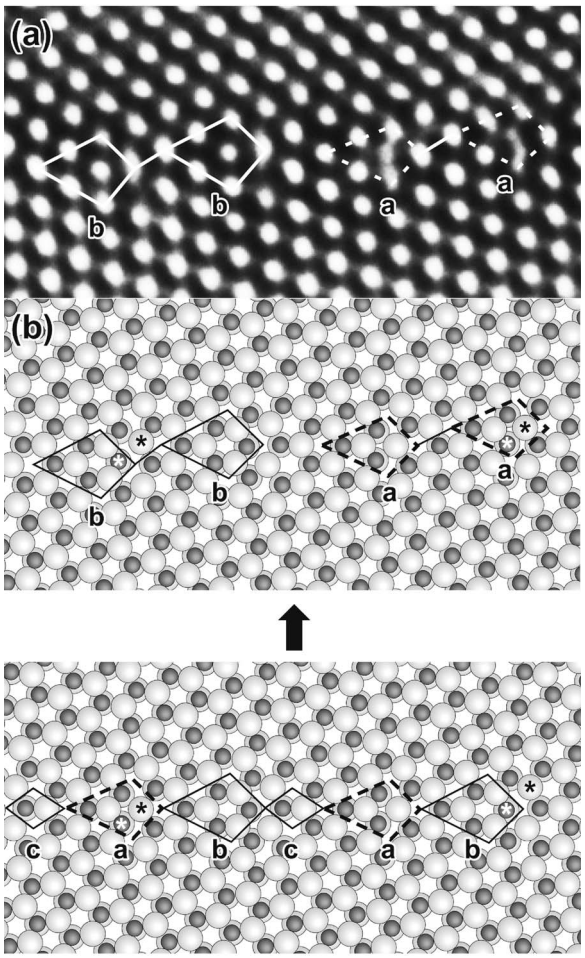

FIG. 8. (a) Enlargements of the experimental HRTEM image, in which a zigzag array of the units is recognized. (b) Atomistic model of structural transition via atom flipping. One of the dislocationlike units becomes the other through the flipping of atomic columns labeled with asterisk. In addition, the straight array is changed to the zigzag array.

the linkage of fivefold- and sevenfold-coordinated open channels, in contrast to eightfold-coordinated open channels in the present study. To make a further conclusion as to why the different atomic structures were observed between GaN and ZnO, further experimental or computational studies would be needed.

B. Zigzag array of the structural units

The $\Sigma=49$ boundary is, thus, found to dominantly consist of a straight array of **a**+**b**+**c**. However, a zigzag array of the units was partly observed in Fig. 5(a). A typical image of such a structure is shown in Fig. 8(a), which is an enlargement of a part of Fig. 5(a). Two dislocationlike units (**b** in the left half and **a** in the right half) are zigzag arrayed. Detailed analysis suggested that the zigzag array is formed as a result of the structural transition from the straight array of **a**+**b**+**c**. As found in previous studies,[48,49] structural transition between **a** and **b** may take place. In the lower panel of Fig. 8(b), a straight array of **a**+**b**+**c** as in Fig. 6(a) is again

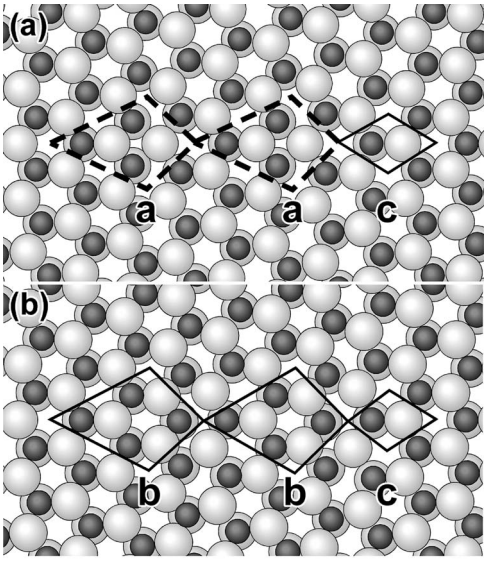

FIG. 9. $\Sigma=49$ boundaries with straight array of the same two dislocationlike units. (a) A boundary with straight array of the units **a**+**b**+**c**. (b) A boundary with straight array of the units **b**+**b**+**c**.

shown. If atomic columns labeled with an asterisk in the left-hand side become farther and debonded and those labeled with an asterisk in the right-hand side become closer and bonded, one of the dislocationlike units will be transformed into the other as shown in the upper part. Subsequently, the straight array will be changed to be the zigzag array. Structural transition via this atom flipping is considered to occur in the $\Sigma=49$ boundary, changing the straight array to the zigzag array.

C. Arrangement of the structural units

As noted in Sec. III A, the present boundary was found to have the characteristic arrangement of two dislocationlike units and a bulklike unit (**a**+**b**+**c**). Here, a question arises: why is such a characteristic arrangement (**a**+**b**+**c**) energetically stable? For example, **a**+**a**+**c** or **b**+**b**+**c** are also possible arrangements of two dislocationlike units and a bulklike unit, since both **a** and **b** are dislocationlike units. Figure 9 shows the calculated structures of **a**+**a**+**c** and **b**+**b**+**c**. Such arrangements (**a**+**a**+**c** and **b**+**b**+**c**) could not be obtained through the simple translation of the half-crystal cell, indicating that these arrangements are not energetically favorable. However, the arrangement of **a**+**a**+**c** in (a) was obtained from the same initial structure as that of **a**+**b**+**c**, where two atomic columns (two Zn and two O) are removed per boundary. Oppositely, **b**+**b**+**c** in (b) was constructed from the same initial structure by adding two columns per boundary. It was found that these two arrangements show higher energies (1.42 J/m^2 for **a**+**a**+**c** and 1.42 J/m^2 for **b**+**b**+**c**) than that for **a**+**b**+**c** given in Fig. 4(a) (1.25 J/m^2).

The preference of **a**+**b**+**c** can be explained by considering local strain in the vicinity of the boundary core. Figures 10(a)–10(c) show the mapping of atomic displacements that occurred during the calculation. Here, displacements indicate atomic movements from the initial structure to the optimized

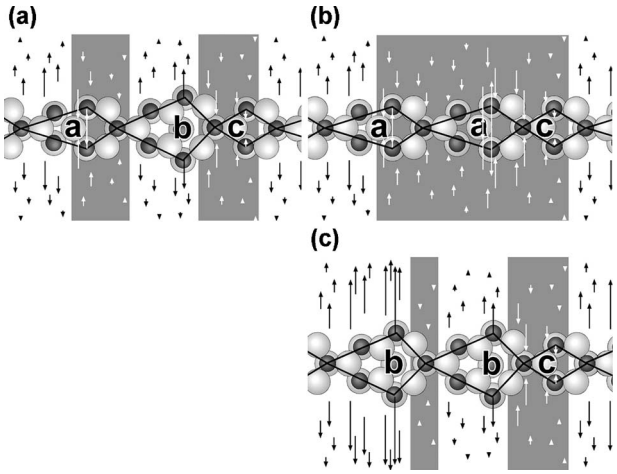

FIG. 10. Maps of atomic displacements in the vicinity of structural units. The arrangement of (a) **a**+**b**+**c**, (b) **a**+**a**+**c**, and (c) **b**+**b**+**c**. Respective arrows indicate atomic displacement in boundary normal direction. Direction and length of the arrows denotes the direction and distance of displacements. Displacements directed toward and opposite to the boundary are denoted by white and black arrows, respectively. Hatches indicate regions where white arrows exist.

one. In the figure, only the displacements in the boundary normal direction are shown, because extensive investigation revealed that displacements in the boundary normal are major components. White and black arrows denote the displacements toward and opposite to the boundary, respectively. Since initial atomic positions are based on ZnO crystal, they should be the optimal condition for ZnO. Thus, displacement from the initial position is considered to induce strain. White arrows indicate that the vicinity of the boundary becomes thinner and vice versa. As a result, white arrows and black ones indicate tensile and compressive strain, respectively.

In **a**+**b**+**c**, the main parts of **a** show tensile strain while the left-hand edges show compressive one. On the other hand, **b** shows compression in the main parts whereas only the right-hand edges show tensile strain. **c** shows compression in the right half and tensile strain in the left half. It seems that compressive and tensile strains are alternatively and similarly formed as a whole. Thus, local strain seems to be effectively relaxed. On the other hand, tensile or compressive strain is dominantly formed in **a**+**a**+**c** or **b**+**b**+**c**. In **a**+**a**+**c**, tensile strain is dominant and compression is formed only in the right half of **c** and the left-hand edge of **a**. Conversely, compression is dominant and tensile is formed only in left half of **c** and the right-hand edge of **b** in **b**+**b**+**c**. The presence of only one kind of strain seems to increase the boundary energies in **a**+**a**+**c** and **b**+**b**+**c**. It is, therefore, considered that the arrangement of **a**+**b**+**c** forms to relax local strain in the vicinity. Such a strain effect may be a critical factor to determine the detailed arrangement of structural units.

The $\Sigma=49$ boundary is, thus, found to consist of a straight array of the units **a**+**b**+**c**. The unit **a** has overcoordinated (fivefold-coordinated) atoms and the unit **b** has undercoordinated (threefold-coordinated) atoms in contrast to fourfold coordination in ZnO bulk. Therefore, the boundary has also a periodic array of under- and overcoordinated atoms along the boundary plane. Such under- and overcoordinated atoms should be related to various grain boundary properties, such as energy, segregation, and electronic states. In addition, undercoordinated atoms may show different effects on the boundary properties from overcoordinated ones. Our previous study indicates the different features in electronic structure between under- and overcoordinated atoms in a ZnO $\Sigma=7$ boundary.[40] The present study on detailed arrangement of structural units gives some guidelines for understanding the coordination and, hence, various boundary properties in oxide materials.

IV. CONCLUSIONS

Detailed arrangement of dislocationlike structural units in the ZnO [0001] $\Sigma=49$ symmetric tilt boundary was investigated. A combination of high-resolution electron microscopy and atomistic calculation revealed that the $\Sigma=49$ boundary is described by the combination of two different dislocationlike units (**a** and **b**) and a bulklike unit (**c**). **a** and **b** are very similar to the structural units found in the $\Sigma=7$ boundary. **a** includes fivefold-coordinated atoms, whereas **b** includes threefold coordination inside the units, in contrast to fourfold coordination in ZnO bulk. Interestingly, the $\Sigma=49$ boundary dominantly consists of a straight array of **a**+**b**+**c**. A zigzag array of the units partly appeared, which can be readily transformed from the straight array via atom flipping at the boundary core. It is considered that a straight array of **a**+**b**+**c** is formed to effectively relax local strain in the vicinity.

ACKNOWLEDGMENTS

We thank Dr. J. D. Gale for allowing us to use the GULP program codes. This work was supported by a Grant-in-Aid for Scientific Research and Special Coordination Funds from the Ministry of Education, Culture, Sports, Science and Technology of Japan. Two of the authors (Y.S. and T.M.) also thank the Japan Society for the Promotion of Science for financial support.

*E-mail: yamataka@k.u-tokyo.ac.jp

[1] K. L. Merkle and D. J. Smith, Phys. Rev. Lett. **59**, 2887 (1987).
[2] F. Ernst, M. W. Finnis, D. Hofmann, T. Muschik, U. Schonberger, U. Wolf, and M. Methfessel, Phys. Rev. Lett. **69**, 620 (1992).
[3] J. D. Rittner and D. N. Seidman, Phys. Rev. B **54**, 6999 (1996).
[4] S. Fabris and C. Elsässer, Phys. Rev. B **64**, 245117 (2001).
[5] V. Potin, P. Ruterana, G. Nouet, R. C. Pond, and H. Morkoç, Phys. Rev. B **61**, 5587 (2000).
[6] I. Dawson, P. D. Bristowe, M.-H. Lee, M. C. Payne, M. D. Segall, and J. A. White, Phys. Rev. B **54**, 13727 (1996).

[7] E. C. Dickey, X. Fan, and S. J. Pennycook, J. Am. Ceram. Soc. **84**, 1361 (2001).
[8] M. Kohyama, Modell. Simul. Mater. Sci. Eng. **10**, R31 (2002).
[9] Y. Ikuhara, T. Watanabe, T. Saito, H. Yoshida, and T. Sakuma, Mater. Sci. Forum **294–296**, 273 (1999).
[10] T. Gemming, S. Nufer, W. Kurtz, and M. Rühle, J. Am. Ceram. Soc. **86**, 581 (2003).
[11] H. Nishimura, K. Matsunaga, T. Saito, T. Yamamoto, and Y. Ikuhara, J. Am. Ceram. Soc. **86**, 574 (2003).
[12] Z. Zhang, W. Sigle, F. Philipp, and M. Rühle, Science **302**, 846 (2003).
[13] K. Matsunaga, H. Nishimura, T. Saito, T. Yamamoto, and Y. Ikuhara, Philos. Mag. **83**, 4071 (2003).
[14] M. F. Chisholm, A. Maiti, S. J. Pennycook, and S. T. Pantelides, Phys. Rev. Lett. **81**, 132 (1998).
[15] Y. Yan, M. F. Chisholm, G. Duscher, A. Maiti, S. J. Pennycook, and S. T. Pantelides, Phys. Rev. Lett. **81**, 3675 (1998).
[16] N. Shibata, F. Oba, T. Yamamoto, and Y. Ikuhara, Philos. Mag. **83**, 2221 (2003).
[17] N. D. Browning, J. P. Buban, H. O. Moltaji, S. J. Pennycook, G. Duscher, K. D. Johnson, R. P. Rodrigues, and V. P. Dravid, Appl. Phys. Lett. **74**, 2639 (1999).
[18] K. L. Merkle and D. Wolf, Philos. Mag. B **65**, 513 (1992).
[19] G. H. Bishop and B. Chalmers, Scr. Metall. **2**, 133 (1968).
[20] G. H. Bishop and B. Chalmers, Philos. Mag. **24**, 515 (1971).
[21] M. J. Weins, H. Gleiter, and B. Chalmer, J. Appl. Phys. **42**, 2639 (1971).
[22] A. P. Sutton and V. Vitek, Philos. Trans. R. Soc. London, Ser. A **309**, 1 (1983).
[23] A. P. Sutton and V. Vitek, *Interfaces in Crystalline Materials* (Oxford University Press, New York, 1995), p. 286.
[24] W. Krakow, Acta Metall. Mater. **40**, 977 (1992).
[25] A. Tsukazaki, A. Ohtomo, T. Onuma, M. Ohtani, T. Makino, M. Sumiya, K. Ohtani, S. F. Chichibu, S. Fuke, Y. Segawa, H. Ohno, H. Koinuma, and M. Kawasaki, Nat. Mater. **4**, 42 (2005).
[26] H. Ohta, M. Orita, M. Hirano, and H. Hosono, J. Appl. Phys. **89**, 5720 (2001).
[27] S. J. Pearton, D. P. Norton, K. Ip, Y. W. Heo, and T. Steiner, J. Vac. Sci. Technol. B **22**, 932 (2004).
[28] R. L. Hoffman, B. J. Norris, and J. F. Wager, Appl. Phys. Lett. **82**, 733 (2003).
[29] F. M. Hossain, J. Nishii, S. Takagi, A. Ohtomo, T. Fukumura, H. Fujioka, H. Ohno, H. Koinuma, and M. Kawasaki, J. Appl. Phys. **94**, 7768 (2003).
[30] D. R. Clarke, J. Am. Ceram. Soc. **82**, 485 (1999).
[31] M. Matsuoka, Jpn. J. Appl. Phys. **10**, 736 (1971).
[32] K. Mukae, K. Tsuda, and I. Nagasawa, Jpn. J. Appl. Phys. **16**, 1361 (1977).
[33] G. E. Pike and C. H. Seager, J. Appl. Phys. **50**, 3414 (1979).
[34] F. Greuter and G. Blatter, Semicond. Sci. Technol. **5**, 111 (1990).
[35] A. N. Kiselev, F. Sarrazit, E. A. Stepantsov, E. Olsson, T. Claeson, V. I. Bondarenko, R. C. Pond, and N. A. Kiselev, Philos. Mag. A **76**, 633 (1997).
[36] J. M. Carlsson, B. Hellsing, H. S. Domingos, and P. D. Bristowe, J. Phys.: Condens. Matter **13**, 9937 (2001).
[37] F. Oba, H. Ohta, Y. Sato, H. Hosono, T. Yamamoto, and Y. Ikuhara, Phys. Rev. B **70**, 125415 (2004).
[38] F. Oba, I. Tanaka, S. R. Nishitani, H. Adachi, B. Slater, and D. H. Gay, Philos. Mag. A **80**, 1567 (2000).
[39] Y. Sato, F. Oba, T. Yamamoto, Y. Ikuhara, and T. Sakuma, J. Am. Ceram. Soc. **85**, 2142 (2002).
[40] Y. Sato, T. Mizoguchi, F. Oba, M. Yodogawa, T. Yamamoto, and Y. Ikuhara, J. Mater. Sci. **40**, 3059 (2005).
[41] J. D. Gale and A. L. Rohl, Mol. Simul. **29**, 291 (2003).
[42] G. V. Lewis and C. R. A. Catlow, J. Phys. C **18**, 1149 (1985).
[43] R. Kilaas, in *Proceedings of the 49th Electron Microscopy Society of America Meeting*, edited by G. W. Bailey (San Francisco Press, 1991), p. 258.
[44] J. M. Cowley and A. F. Moodie, Acta Crystallogr. **10**, 609 (1957).
[45] N. Shibata, F. Oba, T. Yamamoto, and Y. Ikuhara, Philos. Mag. **84**, 2381 (2004).
[46] A. Béré and A. Serra, Phys. Rev. B **66**, 085330 (2002).
[47] J. Chen, P. Ruterana, and G. Nouet, Phys. Rev. B **67**, 205210 (2003).
[48] A. Béré and A. Serra, Phys. Rev. B **65**, 205323 (2002).
[49] F. Oba, Y. Sato, T. Yamamoto, H. Ohta, H. Hosono, and Y. Ikuhara, J. Mater. Sci. **40**, 3067 (2005).